

Pair Interaction Potentials with Explicit Polarization for Molecular Dynamics Simulations of La^{3+} in Bulk Water.

Magali Duvail, Marc Souaille, Riccardo Spezia, and Thierry Cartailleur

Laboratoire Analyse et Modélisation pour la Biologie et l'Environnement,

CNRS UMR 8587, Université d'Evry Val d'Essonne,

Boulevard F. Mitterrand, 91025 Evry Cedex, France.

Pierre Vitorge*

CEA Saclay, DEN/DPC/SECR/LSRM, 91991 Gif Sur Yvette, France.†

Pair interaction potentials (IPs) were defined to describe the La^{3+} - OH_2 interaction for simulating the La^{3+} hydration in aqueous solution. La^{3+} - OH_2 IPs are taken from the literature or parametrized essentially to reproduce *ab initio* calculations at the MP2 level of theory on $\text{La}(\text{H}_2\text{O})_8^{3+}$. The IPs are compared and used with molecular dynamics (MD) including explicit polarization, periodic boundary conditions of $\text{La}(\text{H}_2\text{O})_{216}^{3+}$ boxes, and TIP3P water model modified to include explicit polarization. As expected, explicit polarization is crucial for obtaining both correct La-O distances ($r_{\text{La}-\text{O}}$) and La^{3+} coordination number (CN). Including polarization also modifies hydration structure up to the second hydration shell, and decreases the number of water exchanges between the La^{3+} first and second hydration shells. $r_{\text{La}-\text{O}}^{(1)} = 2.52 \text{ \AA}$ and $\text{CN}^{(1)} = 9.02$ are obtained here for our best potential. These values are in good agreement with experimental data. The tested La-O IPs appear to essentially account for the La-O short distance repulsion. As a consequence, we propose that most of the multi-body effects are correctly described by the explicit polarization contributions even in the first La^{3+} hydration shell. The MD simulation results are slightly improved by adding a –typically negative $1/r^6$ – slightly attractive contribution to the –typically exponential– repulsive term of the La-O IP. Mean residence times are obtained from MD simulations for a water molecule in the first (1082 ps) and second (7.6 ps) hydration shells of La^{3+} . The corresponding water exchange is a concerted mechanism: a water molecule leaves $\text{La}(\text{H}_2\text{O})_9^{3+}$ in the opposite direction to the incoming water molecule. $\text{La}(\text{H}_2\text{O})_9^{3+}$ has a slightly distorted "6+3"

tricapped trigonal prism D_{3h} structure, and the weakest bonding is in the medium triangle, where water exchanges take place.

I. INTRODUCTION

Lanthanide aqueous trications (Ln^{3+}) have similar chemical behaviours. Their hydration structure has been studied by means of classical^{1,2,3,4,5,6,7,8,9,10,11,12,13}, quantum-classical (QM/MM)¹⁴ and Car-Parrinello (CPMD)¹⁵ Molecular Dynamics (MD), and of Monte-Carlo (MC) simulations^{2,16}. Classical Molecular Dynamics (CLMD) simulations can give realistic pictures of hydrated ion structures and dynamics with a relatively low computational cost for simulations up to nanoseconds, a long enough time scale to study exchanges of water molecules in Ln^{3+} first hydration shell. The corresponding Mean Residence Times (MRTs) are out of reach of QM/MM¹⁴ and CPMD¹⁵ simulations. CLMD is now able to settle such time scales using analytical interaction potentials (IPs) that need to be parametrized.

Such IPs can be built to reproduce *ab initio* calculations on systems containing only two molecules, namely actual pair IPs as suggested in two recently published works^{10,11} where different sizes of La^{3+} water clusters were investigated. In Ref.¹⁷ relatively small clusters (up to 9 water molecules with one central Ln^{3+} cation) were studied. Unfortunately, this study did not reproduce the experimental coordination number (CN) of the cation in liquid water, while bigger systems were studied a little later by the same group¹⁰ using another force field which provided better results. To our best knowledge IPs have not been used with explicit polarization and periodic boundary conditions, while such an approach has been limited to big clusters up to 128 water molecules with one central Ln^{3+} cation^{10,11,12}. The advantage of such physical approaches is to provide transferable atomic parameters, since these parameters correspond to atomic intrinsic properties. Nevertheless, in both force fields a short range repulsive term was empirically added^{10,11,12}. When parametrizing their potential for earlier MC simulations Galera *et al.*² have pointed out that the $1/r^{12}$ term in the Lennard-Jones potentials leads to a repulsion that is too strong, whereas the exponential term in the second potential is too weak, albeit a globally good description of structural parameters for lanthanide aqua ions was obtained.

In another approach, the pair IPs have been parametrized to exactly reproduce *ab initio* calculations. For this, many parameters were fitted, but this did not completely re-

produce experimental results of $\text{Ln}^{3+}/\text{H}_2\text{O}$ systems⁸. Pair IPs have also been successfully parametrized to exactly reproduce the available macroscopic experimental results^{9,13}.

Actually, the first pleasing results for Ln^{3+} hydration MD simulations were obtained more than ten years ago by using a pragmatic mixed approach, where the model potentials were tentatively fitted on *ab initio* partial potential energy surfaces, but further rescaled after short time trial simulations by comparison with macroscopic properties^{3,4,5,7}. Polarization effects were taken into account semi-empirically, to be within the reach of MD simulations carried out on 1994's workstations. The polarization procedure was scaled on *ab initio* calculations at the HF level of theory on $\text{Ln}(\text{H}_2\text{O})_8^{3+}$ clusters, and one MP2 calculation⁵. As a result of such a rescaling, the fitting procedure provides phenomenological or bulk rather than actual ion pair, and purely atomic physical parameters. However, such an approach is consistent with the use of well established water models, such as TIP3P, among the most simple ones. For consistency with the rescaling, the *ab initio* calculations were performed on $\text{Ln}(\text{H}_2\text{O})_8^{3+}$ big enough clusters to parametrize the $\text{Ln}^{3+}\text{-OH}_2$ IP, and not only on $\text{Ln}(\text{H}_2\text{O})^{3+}$.

Thus as suggested by literature investigation, MD simulations should explicitly include all polarization effects. They should also be based on $\text{Ln}^{3+}\text{-OH}_2$ IPs parametrized (or checked) in order to reproduce high level quantum calculations of big enough clusters –typically of the $\text{Ln}(\text{H}_2\text{O})_8^{3+}$ size–, so that bulk effects can be correctly described. This because there is no well established theoretical reason for choosing the mathematical form of the repulsion term –typically exponential or $1/r^n$. Supplementary physical terms are usually added as typically $1/r^6$ attractive ones for dispersion; unfortunately, they might as well compensate for systematic errors of the short range repulsion term (because the correct mathematical form of the repulsion term is not undebatable for the interaction of highly charged cations with water). However, the ingredients for realistic MD simulations have not really been put together for a single study on a $\text{Ln}^{3+}/\text{H}_2\text{O}$ system, *i.e.* periodic boundary conditions, explicit polarization and $\text{Ln}^{3+}\text{-OH}_2$ interaction potentials that reproduce high level quantum chemistry calculations. For this reason it is now tempting to gather the above simulation methodologies in a single approach, and to compare the simulation results to well established experimental data. This approach is presented here. For this, we used our own MD code where all these features are implemented¹⁸. An objective of this paper was to test the MD code with a highly charged Ln^{3+} cation, and with a water maximum residence time that can be naturally observed during MD simulations. Thus, different IPs have also been compared.

To simplify the quantum chemistry calculations used to parametrize IPs, we have chosen La^{3+} , the lanthanide with the simplest electronic configuration, *i.e.* closed-shell with no f-electron. It is a chemical analogue of the other lanthanides(III). Lanthanides are essentially stable at the +3 oxidation state, and have similar behaviours in aqueous solutions. This analogy is usually attributed to the hardness of the Ln^{3+} ions: their coordinations mainly depend upon the steric and electrostatic nature of the ligand interactions¹⁹. For the same reason, the 4f-block lanthanide elements are also chemical analogues of the 5f-block actinide elements, when at the same oxidation state^{20,21,22,23,24,25}. Actually, in the nuclear fuel cycle industry, it is a challenge to separate the Am and Cm actinide activation products from (light) lanthanide fission products in an attempt to eliminate long live radionuclides from radioactive wastes. Furthermore, analogies between hard cations at the same oxidation states are currently used as rough estimates for the thermodynamic stabilities of their aqueous hydroxides and complexes with (inorganic) ligands of the underground-waters about possible waste repositories^{25,26,27,28}. The stoichiometries and stabilities of aqueous chemical species are needed to model the solubilities and migrations of radionuclides. The knowledge of hydration is thus the first step needed for the theoretical studies of such chemical reactions.

The La-OH_2 distance ($r_{\text{La-O}}$) is well known in water and has been measured by Extended X-Ray Absorption Fine Structure (EXAFS) Spectroscopy in concentrated Cl^- and ClO_4^- aqueous solutions^{22,29,30,31}. Results are in the 2.54-2.56 Å range. This confirms earlier measurements (2.48 to 2.58 Å) by X-Ray Diffraction (XRD)^{32,33,34}, but with slightly better accuracy. In the treatment of these XRD or EXAFS experimental data, values were fixed or fitted in the range 8 to 12 for the CN of La^{3+} . The $r_{\text{La-O}}$ determinations do not seem to be especially correlated to such CN values, neither to the aqueous concentration of the (Cl^- nor ClO_4^-) counter-anion (less than 2 mol·kg⁻¹). This illustrates that the exact stoichiometry and structure of $\text{La}^{3+}(\text{aq})$ cannot be deduced from such experimental results alone; only, $r_{\text{La-O}}$ is well established being in the range 2.54-2.56 Å.

As outlined above, in published CLMD studies, the IPs have also been built on more qualitative – actually even quite speculative – experimental information and corresponding interpretation. This experimental information has recently been reviewed by Helm and Merbach, see Ref.³⁵ and references therein. From such reviews it is concluded that the stoichiometry of the first La^{3+} hydration shell is $\text{La}(\text{H}_2\text{O})_9^{3+}$ (hence CN = 9), and that the MRT is not known for a water molecule in this first La^{3+} hydration shell. MRTs have been

extracted from ^{17}O NMR measurements only for heavier lanthanides^{3,19,35,36,37,38,39,40}, whose stoichiometry is different ($\text{Ln}(\text{H}_2\text{O})_8^{3+}$). For this reason, such measurements cannot be extrapolated to $\text{La}(\text{H}_2\text{O})_9^{3+}$. However, similar water residence times were found for $\text{Ln}^{3+}(\text{aq})$ and $\text{LnSO}_4^+(\text{aq})$ as extracted from NMR^{37,41,42} and ultrasonic absorption (UA)⁴³ measurements, respectively. For this reason, it has been suggested³⁶ that the residence time in $\text{LaSO}_4^+(\text{aq})$ is a good approximation of that in $\text{La}^{3+}(\text{aq})$, namely 4.8 ns as reinterpreted from an original 1.9 ns value. Nevertheless, this hypothesis needs confirmation, since this analogy (between $\text{Ln}^{3+}(\text{aq})$ and $\text{LnSO}_4^+(\text{aq})$) was only observed when $\text{Ln}^{3+}(\text{aq}) = \text{Ln}(\text{H}_2\text{O})_8^{3+}(\text{aq})$, while experimental data are missing for $\text{Ln}^{3+}(\text{aq}) = \text{Ln}(\text{H}_2\text{O})_9^{3+}(\text{aq})$. Furthermore, shorter residence times are obtained from published MD as compared to the experimental values, as outlined above by Kowall *et al.*⁵ when discussing their pioneering results. The same effect is observed for the later MD published data^{8,10}, when compared with NMR^{36,37,42,44} or UA⁴³ experimental data. The origin of this problem is not clear. For this reason, we will not specially use MRTs to evaluate the quality of simulations. However, we can provide a dynamical picture based on an IP yielding reliable structural data.

The outline of the remainder of the text is as follows. We first describe the model potential forms used (section II A), then the *ab initio* calculations procedure (section II B), and in section II C we present the MD simulation details. Results and discussion are presented in section III, where we first discuss the different potentials used (section III A), and then the influence of the polarization (section III B). Finally the hydration structure of La^{3+} at room temperature (section III C) and its dynamics (section III D) are described.

II. METHODS.

A. Model potentials

The total energy of our system is modelled as a sum of potential energy terms:

$$V_{tot} = V_{elec} + V_{O-O}^{LJ} + V_{La-O} \quad (1)$$

Where V_{elec} is the electrostatic energy term composed of the solvent-solvent and solvent-solute interactions:

$$V_{elec} = \frac{1}{2} \sum_{i,j,i \neq j} \left[\frac{q_i q_j}{r_{ij}} + \frac{1}{r_{ij}^3} (-q_i \mathbf{p}_j + q_j \mathbf{p}_i) \cdot \mathbf{r}_{ij} + \mathbf{p}_i \cdot \overline{\overline{\mathbf{T}}}_{ij} \cdot \mathbf{p}_j \right] + \frac{1}{2} \sum_i \mathbf{p}_i \cdot (\overline{\overline{\alpha}}_i)^{-1} \cdot \mathbf{p}_i \quad (2)$$

where, following the Thole's induced dipole model⁴⁵, each atomic site i carries one permanent charge q_i and one induced dipole \mathbf{p}_i associated with an isotropic atomic polarizability tensor $\overline{\overline{\alpha}}_i$, $\mathbf{r}_{ij} = \mathbf{r}_i - \mathbf{r}_j$,

$$\overline{\overline{\mathbf{T}}}_{ij} = \frac{1}{r_{ij}^3} \left(\overline{\overline{\mathbf{1}}} - 3 \frac{\mathbf{r}_{ij} \mathbf{r}_{ij}}{r_{ij}^2} \right) \quad (3)$$

and $1/2 \sum_i \mathbf{p}_i \cdot (\overline{\overline{\alpha}}_i)^{-1} \cdot \mathbf{p}_i$ is the polarization energy. As previously mentioned we used the Thole's model where the polarization catastrophe is avoided using a screening function for the dipole-dipole interactions at short distances. Here we adopted the exponential form among the originally proposed screening functions because of its continuous character (also shared by its derivatives), so that the electrostatic potential is now

$$V_{elec} = \frac{1}{2} \sum_{i,j,i \neq j} (q_i + \mathbf{p}_i \cdot \nabla_i) (q_j - \mathbf{p}_j \cdot \nabla_j) \phi^s(r_{ij}) + \frac{1}{2} \sum_i \mathbf{p}_i \cdot (\overline{\overline{\alpha}}_i)^{-1} \cdot \mathbf{p}_i \quad (4)$$

where $\phi^s(r_{ij})$ is the screened electrostatic potential

$$\phi^s(r_{ij}) = \frac{1}{r_{ij}} \left[1 - \left(1 + \frac{au}{2} \right) e^{-au} \right] \quad (5)$$

with $u = r_{ij}/(\alpha_i \alpha_j)^{1/6}$ and $a = 2.1304 \text{ \AA}^{-1}$ as determined in the original work⁴⁵. Isotropic polarizabilities are assigned at each atomic site. Here we used atomic polarizabilities determined by van Duijnen *et al.*⁴⁶ for O (0.85 \AA^3) and H (0.41 \AA^3) and for La^{3+} the tabulated value⁴⁷ of 1.41 \AA^3 (see Tab. I). The induced dipoles are obtained through the resolution of the self-consistent equations

$$\mathbf{p}_i = \overline{\overline{\alpha}}_i \cdot \left(\mathbf{E}_i + \sum_{i \neq j} \overline{\overline{\mathbf{T}}}_{ij} \cdot \mathbf{p}_j \right) \quad (6)$$

The resolution of this self-consistent problem becomes rapidly extremely time-consuming as the system grows. In order to reduce computing time, we have used an alternative way of

resolving such a problem for each time step of the dynamics. In particular, we have used a Car-Parrinello type of dynamics⁴⁸ of additional degrees of freedom associated with induced dipoles⁴⁹. Thus, the Hamiltonian of the system is now

$$\mathcal{H} = V + \frac{1}{2} \sum_i m_i \mathbf{v}_i^2 + \frac{1}{2} \sum_i m_{\mathbf{p}_i} \mathbf{v}_{\mathbf{p}_i}^2 \quad (7)$$

where V is the total potential, \mathbf{v}_i is the velocity of the atom i , $\mathbf{v}_{\mathbf{p}_i}$ is the velocity of the induced dipole \mathbf{p}_i treated as an additional degree of freedom in the dynamics and $m_{\mathbf{p}_i}$ is its associated fictitious mass (identical for each atom). Dynamics of the induced dipoles degrees of freedom is fictitious, such that it only serves the purpose of keeping the induced dipoles close to their values at the minimum energy (that would be obtained through the exact resolution of self-consistent equations). Thus, induced dipoles dynamics adiabatically follows the nuclei dynamics if a proper choice of the fictitious mass is done. A decoupling, or at least a very weak coupling, between nuclei degrees of freedom and fictitious dipole degrees of freedom is needed to maintain adiabaticity. Fictitious masses are connected to characteristic frequencies of the induced dipoles

$$\omega_{\mathbf{p}_i} = \frac{2\pi}{\tau} = \frac{1}{\sqrt{m_{\mathbf{p}_i} \alpha_i}} \quad (8)$$

that are set here to be $\tau = 0.005$ ps for each atomic site. Further details are given in Ref.¹⁸.

V_{O-O}^{LJ} in Eq. 1 is the 12-6 Lennard-Jones (LJ) potential⁵⁰ describing the O-O interaction of TIP3P water molecules⁵¹.

$$V_{ij}^{LJ} = \sum_{i,j} 4\epsilon_{ij} \left[\left(\frac{\sigma_{ij}}{r_{ij}} \right)^{12} - \left(\frac{\sigma_{ij}}{r_{ij}} \right)^6 \right] \quad (9)$$

The partial atomic charges in O and H of the original TIP3P water model had been optimised to reproduce water properties based on models without polarization⁵¹, containing only an electrostatic term and a 12-6 LJ term. Introducing a polarization term in the model will over-estimate the water dipole moment. Consequently, a scaling factor is introduced on the partial atomic charges to reproduce the experimental dipole moment of water as done by Caldwell et al.^{52,53} and Armunanto et al.⁵⁴. By recalculating this scaling factor, we obtained atomic partial charges on O and H of $-0.658e$ and $+0.329e$ respectively (Tab. I). This model

is here called the TIP3P/P model. Namely, two water models were used: (i) the TIP3P/P model including the V_{pol} term, and (ii) the original TIP3P model when polarization term is not added on the electrostatic interaction, *i.e.* in the latter case the electrostatic term is only composed of a Coulomb term.

V_{La-O} account for the *non-electrostatic* La-O interactions. Several potential forms were tested to describe these interactions. First the purely repulsive exponential (Exp) potential,

$$V_{ij}^{Exp} = A_{ij}^{Exp} \exp(-B_{ij}^{Exp} r_{ij}) \quad (10)$$

where A_{ij}^{Exp} and B_{ij}^{Exp} are fitted parameters. Then the Buckingham exponential-6 (Buck-6) potential⁵⁵,

$$V_{ij}^{Buck6} = A_{ij}^{Buck6} \exp(-B_{ij}^{Buck6} r_{ij}) - \frac{C_{6,ij}^{Buck6}}{r_{ij}^6} \quad (11)$$

where the fitted parameters are A_{ij}^{Buck6} , B_{ij}^{Buck6} and $C_{6,ij}^{Buck6}$. And finally the Tosi-Fumi (TF) potential^{56,57},

$$V_{ij}^{TF}(r_{ij}) = A_{ij}^{TF} \exp(-B_{ij}^{TF} r_{ij}) - \frac{C_{6,ij}^{TF}}{r_{ij}^6} - \frac{C_{8,ij}^{TF}}{r_{ij}^8} - \frac{C_{10,ij}^{TF}}{r_{ij}^{10}} \quad (12)$$

where the fitted parameters are A_{ij}^{TF} , B_{ij}^{TF} , $C_{6,ij}^{TF}$, $C_{8,ij}^{TF}$ and $C_{10,ij}^{TF}$. For these three La-O IPs, the parameters were fitted on MP2 *ab initio* calculations of $\text{La}(\text{H}_2\text{O})^{3+}$ and/or $\text{La}(\text{H}_2\text{O})_8^{3+}$, and eventually refined on MD simulations (see Sections II B and III A for details). The resulting values are shown in Tab. I. We also tested the Kitaygorodsky (Kit) potential⁵⁸ describing both La-water and the water-water *non-electrostatic* interactions:

$$V_{int}^{Kit} = \sum_i \sum_j k_i \cdot k_j \left(G_{ij} C \exp(-\gamma z) - \left(\frac{C_6}{z^6} + \frac{C_8}{z^8} + \frac{C_{10}}{z^{10}} \right) + G_{ij} C^{de} \exp(-\gamma^{de} z) \right) \quad (13)$$

where

$$z = \frac{r_{ij}}{r_{ij}^0} \quad (14)$$

and

$$r_{ij}^0 = \sqrt{(2R_i^w)(2R_j^w)} \quad (15)$$

where R_i^w and R_j^w are the van der Waals radii. Here, the numerical values of the parameters are assumed to reflect actual atomic properties, for this reason they should be fitted on various molecules. Here we have used the original Derepas parameters^{17,59}. In the Kit

expression

$$G_{ij} = \left(1 - \frac{q_i}{n_i^{val}}\right) \left(1 - \frac{q_j}{n_j^{val}}\right) \quad (16)$$

where q_i is the partial atomic charge of atom i and n_i^{val} is the number of valence electrons of atom i . Note that parameters C_6 , C_8 , C_{10} , C , C^{de} , γ and γ^{de} are independent from the atomic species i and j (Tab. I). For best comparing only the Kit La-O IP with our potentials, we performed simulations with (i) the Kit potential for all interactions, and (ii) the Kit only for the La^{3+} -O interaction and the TIP3P/P model for the O-O water interactions. This modified Kit potential is here called Kit-TIP3P/P potential.

We have also tested a 12-6 LJ potential (Eq. 9) for the La-O IP. This gave poor results, and we finally did not use this kind of potential for the La-O interaction.

B. *Ab initio* calculations

The La-O interaction energies fitted by using the analytic functions described in Sec. II A were obtained from calculated *ab initio* Potential Energy Surfaces (PES) scan. Symmetric model $\text{La}(\text{H}_2\text{O})_8^{3+}$ clusters were built (Fig. 1), where the La-O distances were equal for the eight water molecules. The La-O distance was scanned with fixed TIP3P water geometry.

Ab initio calculations were performed using the Gaussian-98 package⁶⁰. The PES scan was performed at the second-order Møller-Plesset perturbation (MP2) level of theory. The La atom was described by the LanL2MB basis set and its associated pseudopotential^{61,62,63}. Hydrogen and oxygen atoms were described by the 6-31G* basis set⁶⁴. As usual, the size of the chosen basis set is a compromise between accuracy of electronic calculation and the size of the clusters used to parametrize or check the La-O potential, namely this level of theory allowed *ab initio* calculations on a $\text{La}(\text{H}_2\text{O})_{24}^{3+}$ cluster.

C. Molecular dynamics simulations.

a. Simulation details. Simulations of the hydrated La^{3+} ion have been carried out in the microcanonical *NVE* ensemble with our own developed CLMD code¹⁸. CLMD simulations were performed for one La^{3+} and 216 rigid water molecules in a cubic box at room temperature. A few tests with a larger simulation box (1000 water molecules) were performed. It gave virtually the same results, so that all the following reported results are for

the former simulation box.

Periodic boundary conditions were applied to the simulation box. Long-range interactions have been calculated by using Smooth Particle Mesh Ewald (SPME) method⁶⁵. The coulombic energy divergence catastrophe is avoided by a *neutralizing plasma*^{66,67} implemented in Ewald summation by omitting the $\mathbf{k} = 0$ term in the reciprocal space sum⁶⁸. The net-charge of the system induces a charged system term ($U_c = |\sum_i^N q_i|^2 / (8\epsilon_0 V \alpha^2)$)⁶⁹. In our case, this term results in adding a constant contribution to the total energy (since the net-charge q , and the volume V , are constant in our simulations) corresponding to 0.2 % of the total energy. However, the corresponding forces are not affected by this charged system term. Simulations were performed using a Velocity-Verlet-Based Multiple Time Scale (MTS) for the simulations with the TIP3P/P water model. Equations of motion were numerically integrated using a 1 fs time step. The system was equilibrated at 298 K for 2 ps. Production runs were subsequently collected for 3 ns. Computing time for each 3 ns trajectory varied from 21 hours without explicit polarization to 30 hours with explicit polarization on a 2.4 GHz AMD Opteron CPU. The average temperature was 299 K with a standard deviation of 10 K. To check that the system was correctly thermalised, we have performed simulations at different temperatures (within the liquid water domain). This gave linear van't Hoff plots for the $\text{La}(\text{H}_2\text{O})_{i-1}^{3+}/\text{La}(\text{H}_2\text{O})_i^{3+}$ water exchange reactions of the first hydration shell. This reflects negligible heat capacity influence, and thus correct thermalisation of the system. However, temperature influence is out of the scope of the present paper, and will be published elsewhere⁷⁰.

b. Radial Distribution Function (RDF) La-O and La-H RDFs were determined for the first and the second hydration shells; the CN is obtained by integrating the RDF:

$$CN = 4\pi\rho \int_{r_{min}}^{r_{max}} g(r)r^2 dr \quad (17)$$

where r_{min} and r_{max} are the first and the second minima of the RDF, respectively, and ρ the atomic density of the system.

c. Mean residence time of water molecules The Impey procedure⁷¹ is generally used to determine the MRT of ligands when all ligands of a given shell have been exchanged. As the MRT of water molecules with Ln^{3+} ions is quite long (about 1 ns for La^{3+} at room temperature¹⁰), the “direct” method⁷² was used to determine the MRTs of water molecules.

The MRTs were thus estimated from an average of the time spent by a water molecule in the first hydration shell. As in the Impey procedure, a minimum time parameter ($t^*=2.0$ ps) defining a real “exchange” was introduced. For consistency, the same protocol was used to estimate the MRTs for the second hydration shell.

III. RESULTS AND DISCUSSION.

A. Comparison of La-O interaction potentials

Three potentials were parametrized (see Section II A): Exp (Eq. 10), Buck-6 (Eq. 11) and TF (Eq. 12), while the Kit and Kit-TIP3P/P (Eq. 13) potentials were used with published parameters (see Section II A). MD simulations were performed at room temperature with these potentials and explicit polarization. These results are here first compared with available published r_{La-O} experimental values, and to expected CN = 9 (Tab. II). We will give more details on Buck-6 MD simulations (*i.e.* MD simulations using the Buck-6 potential), because it gives the best results (among our parametrized potentials), while the other ones (Exp, TF, Kit and Kit-TIP3P/P) were used for comparison.

Quite surprisingly, the simplest (Exp) La-O pair IP gave relatively good results: $r_{La-O}^{(1)} = 2.59$ Å to be compared with 2.54^{22} and 2.56^{29} Å average La-O distance obtained by EXAFS spectroscopy (Tab. II). The CN = 8.77 calculated coordination number is of the correct order of magnitude. The Exp potential was parametrized only on *ab initio* calculations of $La(H_2O)^{3+}$, since this potential form cannot reproduce the shape of the energy curves of the bigger $La(H_2O)_8^{3+}$ clusters, where a slightly attractive contribution is present in the 2.5 - 5.0 Å La-O distance range. Unfortunately, exponential function cannot account for such negative contributions. Nevertheless, note that the good results of the MD simulations indicate that polarization is enough to account for most of the multi-body attractive effects, since Exp was parametrized on the $La^{3+}-OH_2$ two-body system.

For the previously mentioned reasons we kept the exponential repulsive term, and added an $(-1/r^6)$ attractive term: this is the Buck-6 potential. We fitted all the parameters, now also using $La(H_2O)_8^{3+}$ clusters. For this reason, these parameters also account for short range multi-body effects. We then further slightly refined the parameters by using trial MD

simulations. The obtained Buck-6 La-O distance (2.52 Å) is in reasonable agreement with published EXAFS results (2.54²² and 2.56²⁹ Å), and with a recent MD value obtained for La(H₂O)₆₀³⁺ clusters (2.56 Å¹⁰). The CN (9.02) of the first hydration shell is also in good agreement with experimental evidence and with the CN (8.9) obtained by Clavaguera *et al.*¹⁰ in their MD study of La(H₂O)₆₀³⁺. Note that they have used a 14-7 repulsive-dispersion term, while we used an exponential-6 one.

The minimum energy of the La³⁺-OH₂ two-body system is at about 2.3 Å, while the Buck-6 potential is slightly attractive for distances greater than 2.6 Å. However, at these distances the Buck-6 potential energy is less than 10 % of the total energy, and less than 6 % at distances more than 4 Å, that correspond to the beginning of the second hydration shell (Fig. 2). This confirms that most of the multi-body effects are in the explicit polarization term, and not in fitted parameters. Namely La-water polarization energy is 42, 43 and 23 % of the total energy at 2.3, 2.6 and 4 Å respectively, while for water - water interaction it is about 5 to 10 % of the total interaction⁷³. The Buck-6 potential is an important contribution term to the total energy only at very short distances. It accounts for repulsion. Since the 1/r⁶ term is here attractive, most of this attraction is more of physical origin, *i.e.* dipole-dipole interactions rather than an empirical term for compensating the exponential one. This results in an overall attractive Buck-6 potential at the distances indicated just above. This is in contrast with the always positive Kit IPs (Eq. 13). Nevertheless, for both (Buck-6 and Kit) potentials the exponential term is shifted (by about 0.14 and 0.07 Å respectively) to larger distances as compared to the overall repulsion wall. This might very well reflect that the (1/rⁿ) attractive(s) term(s) are also partially correcting the shape of the repulsive term, because its (exponential) form is not completely appropriate.

By comparing now the MRTs of water molecules in the first hydration shell, the Buck-6 potential appears to give a MRT five time greater than that obtained with the Exp potential. Actually, the first peak of the La-O RDF obtained with the Buck-6 potential is narrower and more symmetric than that obtained with the Exp potential (Fig. 2). This reflects that water molecules are more strongly bounded to La³⁺ and less likely to exchange when using the Buck-6 potential.

The TF potential provided quite poor results. It over-estimates the La-O distance of the first hydration shell by about 0.1 Å. It also over-estimates the CN (see Tab. II). Attempts to slightly refine these parameters (as done for the Buck-6 potential) did not improve the MD

simulation results much. It might seem surprising that adding terms to Buck-6 for obtaining TF and refitting all of them did not improve the model. Actually, this is originated in the fitting, which results now in a $C_{6,ij}^{TF}/r^6$ repulsive term ($C_{6,ij}^{TF} < 0$). We did not attempt to add further constraints in the fitting procedure, as typically $C_{6,ij}^{TF} > 0$, because the Kit potential already has an attractive $1/r^6$ term (see below) and then we can only recover this potential. Furthermore, the TF potential has the most important attractive contribution among the tested potentials. This is rather a consequence of the incorrect mathematical form of the main repulsion term, which explains the poor results obtained with the TF potentials. Note that repulsive $C_{6,ij}$ terms are quite common and can provide good TF potentials for doubly charged transition metals⁷⁴.

In conclusion, among our three potentials, – *i.e.* the Exp, the Buck-6 and the TF potentials – MD simulations using the Buck-6 potential with explicit polarization better reproduces available well established experimental information.

The Buck-6 potential is now compared with the published Kit¹⁷ and the Kit-TIP3P/P potentials (Tab. II). The analytical expression of the Kit potential is similar to that of the TF potential, since the dispersion-exchange term is negligible as compared to the repulsion and dispersion terms. However, the La-O distances and the CNs obtained for the first hydration shell by using the Kit and the Kit-TIP3P/P potentials are different from those obtained by using the TF potential. The La-O distance obtained with the Kit potential (2.55 Å) is in very good agreement with experimental values for the first hydration shell (Tab. II), whereas a La-O distance of 2.65 Å was calculated with the TF potential. Note that we did not optimise the Kit potential parameters: we took published values for C_6 , C_8 , C_{10} , C , C^{de} , γ and γ^{de} (see Sec. II A), which, in principle, reflect atomic properties. This might mean that they were not specially fitted on $\text{La}^{3+}/\text{H}_2\text{O}$ *ab initio* results. The Kit potential is thus only defined by a repulsion-dispersion term depending essentially on the van der Waals radii of interacting species. The Kit La-O IP curve appears to be between the Exp and Buck-6 ones for $\text{La}(\text{H}_2\text{O})^{3+}$ (data not shown). Note that the Exp, Buck-6 and Kit potentials give similar MD results for the structural properties of the first hydration shell (Tab. II). Furthermore, the Kit MRT is of the same order of magnitude as the Exp MRT, *i.e.* 200 ps. It is about five times smaller than the Buck-6 MRT.

The difference might be originated in the La-O IP or from the water model. To check this, the TIP3P/P water model was used, namely MD simulations were performed by using

the Kit-TIP3P/P potential. Indeed, instead of describing the O-O IP with the Kit potential, the O-O interaction was described with the TIP3P/P. This changed MD simulation results (Tab. II). Namely, the Kit O-O RDF is composed of two peaks centred at 2.82 Å and at about 6.60 Å, while the Kit-TIP3P/P model gives three O-O RDF peaks at 2.70, 4.80 and about 6.80 Å (Fig. 3). These last results are in good agreement with neutron diffraction results obtained for liquid water at 298 K⁷⁵. The repulsion term of the Kit potential for the water-water interaction is more important than that of the 12-6 LJ potential describing the water-water interaction in liquid water. The difference in the repulsion between the two models is also reflected in the MRTs values for the first hydration shell, *i.e.* the Kit MRT is twice smaller than the Kit-TIP3P/P MRT. It appears that the Kit-TIP3P/P and the Buck-6 MD simulations provide the closest results as compared to those using the other tested potentials. Thus, the Buck-6 and the Kit-TIP3P/P potentials are the potentials providing better agreement with experimental data among the five potentials tested to simulate the La³⁺ hydration in aqueous solution with explicit polarization.

The Buck-6 and Kit-TIP3P/P potentials nevertheless give slightly different results for the second hydration shell: the Buck-6 MD simulations provide a slightly smaller second hydration shell La-O distance and CN. Compared with experimental data $r_{La-O}^{(2)}$, the Buck-6 value (4.65 Å) is closer to recent EXAFS (4.63 Å)²⁹ and older XRD (4.70 Å)³² data, than the Kit-TIP3P/P one (4.78 Å). These small differences are also reflected in MRT⁽¹⁾, the water residence time in the first La³⁺ hydration shell. MRT⁽¹⁾ is correlated to the water exchange mechanism, which involves the second hydration shell. It is important to notice that the Buck-6 potential has a simple analytical form that will allow us to easily extrapolate our results to other lanthanides. To illustrate that, we used published ionic radii⁷⁶ in an attempt to extrapolate the La-O Buck-6 parameters to the other lanthanides; *i.e.* we changed parameters to visually shift the La-O IP by the difference between the ionic radii. The corresponding MD simulations reproduced published r_{Ln-O} distances, and the decrease in CN with atomic number in the Ln series (from CN = 9 to 8)⁷⁷.

Finally, we chose the Buck-6 potential as our favorite potential since it provides correct structural and dynamical informations and can be extended to other atoms in the lanthanide series. Its validity was further evaluated by comparing the *ab initio* (MP2) and model calculated energies of small clusters, *i.e.* (La-OH₂)_n³⁺ with n=1,2,3,8, and bigger clusters extracted from MD simulations, (La-OH₂)_n³⁺ (H₂O)_m with n=8 or 9 and n+m = 9,14,24

(Fig. 4). A good agreement between the MP2 and model energies is obtained for all the studied clusters with negative energies (Fig. 5). Some points are not on the $E_{model} = E_{ab initio}$ line: they correspond to positive energies calculated in the repulsion walls. We indeed endeavoured to reproduce the energies corresponding to La-O distances more than 2 Å, since the closest observed La-O distance was 2.20 Å in our MD simulations at 299 K. Moreover, this comparison shows that the correlation between MP2 and model energies is better when increasing the number of water molecules, e.g. the relative difference between model and *ab initio* energies is of 0.6 % for the $\text{La}(\text{H}_2\text{O})_{24}^{3+}$ cluster. This also confirms the good transferability of the TIP3P/P water model together with the reliability of the implemented polarization. In conclusion, increasing the number of water molecules improves the correlation between MP2 and model energies. The Buck-6 potential is thus appropriate to correctly describe the La-O interaction for simulations of La^{3+} in aqueous solution.

B. Polarization effects

As for the TIP3P/P water model, we compared several potential forms to describe the La-O interaction without explicit polarization, and with the TIP3P water model (see Sec. II A), *i.e.* the Exp_{up} , the Buck-6_{up} and the TF_{up} potentials, where subscript *up* is for unpolarizable. For the Exp_{up} potential a La-O distance of 2.46 Å and a CN of 9 were found for the first hydration shell (Tab II). The second hydration shell is centred at 4.60 Å with 18 water molecules: only the first shell is really incorrect, it is too small by at least 0.06 Å. For the Buck-6_{up} potential, we have obtained a La-O distance of 2.56 Å and a CN of 10 (instead of the expected value of 9) for the first hydration shell, and a La-O distance of 4.70 Å with 20 water molecules for the second hydration shell. For the TF_{up} potential a La-O distance of 2.62 Å is obtained and a CN of 12 for the first hydration shell, and a La-O distance of 4.75 Å and a CN of 26 for the second hydration shell. The results obtained with the TIP3P water model (Tab. II) are not consistent with those obtained with the TIP3P/P model, neither with experimental data. The Buck-6_{up} potential is the only potential that gives results in good agreement with experimental La-O distance^{22,29}. However, with this potential, the CN is too large, *i.e.* a CN of 10 instead of 9. On the other hand, the Exp_{up} potential gives a consistent CN for the first hydration shell, as compared to the experimental and computed CN, but the calculated La-O distance is too small, *i.e.* the La-O distance is under-estimated

by about 0.1 Å. The TF_{up} does not give correct results at all (Tab. II). In conclusion, without explicit polarization we did not succeed to reproduce both correct distance and CN for the first hydration shell.

This strengthens the view that polarization holds an important role in the hydration of La^{3+} , and this is poorly accounted for by fitting pair IPs. Taking into account polarization explicitly is thus essential to describe correctly the hydration of La^{3+} in aqueous solution.

C. Structural properties

Here we describe in some details structural properties obtained with the Buck-6-TIP3P/P model. La-O RDF shows two well-defined peaks corresponding to the first and the second hydration shells (Fig. 6.a.). The first and second peaks are centred at 2.52 Å and at 4.65 Å respectively (Tab. II), while the third hydration shell is not well-defined. As the other hydration shells are not defined, we can conclude that La^{3+} has an effect only on the first three hydration shells (to about 8 Å). At 299 K, the calculated La-O distance of the first hydration shell is in good agreement with experimental and computed values shown in Tab. II. The mean associated coordination number of 9.02 is an average of different distribution complexes with CN = 9 and 10. CN = 9 is the most frequent, *i.e.* 98.1 % and 1.9 % for $La(H_2O)_9^{3+}$ and $La(H_2O)_{10}^{3+}$ respectively. Also the La-O distance and coordination number of the second hydration shell, *i.e.* 18.8 water molecules at 4.65 Å, are consistent with the experimental and computed values (Tab. II) as already outlined above. Angular distribution function (ADF) of O-La-O shows two peaks (Fig. 6.b.). The first peak is located at 70° and the second at 137°. ADF obtained from MD simulations is consistent with ADF obtained for $La(H_2O)_9^{3+}$ complex in the D_{3h} tricapped trigonal prism (TTP) geometry (Figs. 4.a.b.). Fitting the La-O distances of the first hydration shell with two gaussian distribution functions, two La-O distances of 2.50 and 2.58 Å (with corresponding CNs 6 and 3) have been calculated, corresponding to two different water molecules populations: the capping (3) and the prismatic (6) water molecules. ADF is also in good agreement with ADF for a TTP geometry obtained by Chaussedent et al.⁷⁸ for their MD study of Eu^{3+} in aqueous solution.

The La-H peak of the first hydration shell is centred at 3.17 Å. The number of H in the first hydration shell is of 18.5 corresponding to about twice the number of water molecules in the first shell. It is less straightforward to determine the limit of the second hydration

shell from La-H RDF, since the two corresponding peaks are not entirely separated.

The La-O and CN results we obtained by using the Buck-6 potential for the second hydration shell (Tab. II) are consistent with experimental data obtained by Large Angle X-Ray Scattering (LAXS) spectroscopy²⁹, *i.e.* a La-O distance of 4.63 Å and a CN of 18.

D. Dynamical properties

Water exchanges between the first and the second hydration shells obtained with Buck-6-TIP3P/P MD simulations are observed and detailed in what follows (16 water exchanges). The main reaction is the synchronous leaving and incoming of a water molecule (Fig. 7). A transient complex $\text{La}(\text{H}_2\text{O})_{10}^{3+}$ is observed during the exchange with a lifetime of up to 10 ps. The starting species is $\text{La}(\text{H}_2\text{O})_9^{3+}$ of approximately tricapped trigonal prism TTP D_{3h} structure composed of three parallel triangles. The top and bottom ones are symmetric, while the medium one is a little bigger and in opposition (rotation of 60°) to the two other ones. For this reason, this structure can be named "6+3". Note that looking to a rectangle face of TTP, it can also be seen as a deformed D_{4d} square antiprism (SAP), the classical "2x4" geometry of $\text{Ln}(\text{H}_2\text{O})_8^{3+4}$ with the ninth water molecule outside the centre of one face, a "2x4+1" or "4+(4+1)" geometry. In the medium triangle, the La-O distances are slightly bigger (Tab. II), corresponding to weaker bonds. Indeed, the exchanges are observed in this medium plane. The O_{in} -La- O_{leav} angle is about 180°, when the incoming water molecule (H_2O_{in}) is arriving and the leaving one ($\text{H}_2\text{O}_{leav}$) is still here. Resulting $\text{Ln}(\text{H}_2\text{O})_{10}^{3+}$ have a deformed D_{4d} SAP structure, *i.e.* the classical geometry of $\text{Ln}(\text{H}_2\text{O})_8^{3+}$ with now two supplementary water molecules outside the centre of each square, a "2x(4+1)" geometry. These two extra-molecules are actually the incoming and leaving water molecules. When the leaving water molecule has gone away, $\text{Ln}(\text{H}_2\text{O})_9^{3+}$ comes back to TTP geometry.

Helm *et al.*³⁵ suggested a dissociative interchange for water exchanges on $\text{Nd}(\text{H}_2\text{O})_9^{3+}$, *i.e.* a concerted exchange with a weak dissociative character, via a $\text{Nd}(\text{H}_2\text{O})_8^{3+}$ transient complex. However, the water exchanges reaction pathway for lanthanide ions is not clearly defined^{7,19,35,40}. Moreover, the reaction pathway we have observed could not be compared to the one suggested by Helm *et al.* since the two main configurations we have observed are $\text{La}(\text{H}_2\text{O})_9^{3+}$ and $\text{La}(\text{H}_2\text{O})_{10}^{3+}$, while the reaction pathway proposed by Helm *et al.* is for the $\text{Nd}(\text{H}_2\text{O})_9^{3+} / \text{Nd}(\text{H}_2\text{O})_8^{3+}$ exchange.

The calculated MRT of water molecules at 299 K is about 1 ns (Tab. II). Unfortunately, there are no experimental data of water molecules MRT in aqueous solution of La^{3+} to compare with as already outlined in Introduction. Water exchange rate constants have been extracted from ^{17}O NMR measurements of Ln^{3+} aqueous solutions^{3,19,35,36,37,38,39,40}. These rate constants appeared to decrease with the atomic number. Unfortunately, it could only be measured for heavy lanthanides, whose structure is $\text{Ln}(\text{H}_2\text{O})_8^{3+}$. The kinetic effect is indeed not sufficient to enable the determination of water exchange rate constants for light lanthanides ($\text{Ln} = \text{La} - \text{Sm}$)^{5,35}. For this reason, extrapolation down to light $\text{Ln}(\text{H}_2\text{O})_9^{3+}$ species is highly hypothetical. Nevertheless, few authors proposed such extrapolation assuming a maximum value of the exchange rate constant, and consequently a minimum value of MRT, for Gd^{3+} ³⁵. The ^{17}O NMR MRTs published for 9-coordinated Ln^{3+} are 2 ns ($\text{Pr}(\text{H}_2\text{O})_9^{3+}$) and 2.5 ns ($\text{Nd}(\text{H}_2\text{O})_9^{3+}$)³⁵, 943 ps³⁷ and 833 ps⁴⁰ ($\text{Gd}(\text{H}_2\text{O})_9^{3+}$), and 2.02 ns ($\text{Tb}(\text{H}_2\text{O})_9^{3+}$)^{37,79,80}. These values indicate that MRTs are of one to few ns. A MRT of 980 ps has been obtained for a 1 ns MD simulation on a $\text{La}(\text{H}_2\text{O})_{60}^{3+}$ cluster¹⁰, a value very similar to the one we obtained. Nevertheless, experimental confirmations are still needed.

IV. CONCLUSIONS AND OUTLOOKS

This work, as can be argued by a careful literature examination, clearly shows that explicit polarization is needed for studying La^{3+} in liquid water by means of CLMD simulations, and that the parametrized La-O interactions should reproduce high level *ab initio* calculations, preferably on clusters with realistic multi-body effects. However, to our best knowledge, these methodologies have not been used in a single study based on MD simulations with periodic boundary conditions to correctly simulate a liquid system. Taking into account all these aspects, we were able to correctly reproduce available experimental data, this strengthening the confidence in our approach and more precisely in pair IP energy forms and related parameters when combined with explicit polarization. Note that we used a simple model for water (TIP3P/P) and fixed atomic partial charges. Furthermore, we obtained from simulations supplementary insights on La^{3+} hydration for which there is still not undebated experimental information.

In the present work, several La-O IPs were parametrized in order to simulate the hydration of La^{3+} in aqueous solution: the Exp, Buck-6 and TF potentials. The Buck-6 potential is

slightly negative in the 2.6 - 4.2 Å range for the two body $\text{La}(\text{H}_2\text{O})^{3+}$ system. We should notice that potentials lacking this attractive contribution (Exp or Kit-TIP3P/P) are also able to provide reasonable results for the first hydration shell structure. The main difference is in the second hydration shell and associated properties, in particular MRTs. The attractive contribution of Buck-6 is associated with longer water residence times in the La^{3+} first hydration layer. That seems more in agreement with experimental information.

Most of the many-body effects were taken into account by explicit polarization, which was confirmed to be needed for reproducing both well established distances and CNs. Explicit polarization essentially decreases – and improves – the MD modelled La^{3+} first hydration shell coordination number, and slightly decreases the size of the second hydration shell. It also increases the water molecule MRT in the first La^{3+} hydration shell. Note that other MD residence times obtained with other potentials described in this work are smaller and indeed probably too small. This reflects differences in the second hydration shell among MD results. We observed that the residence time is essentially originated in the transient formation of $2 \times (4+1) \text{La}(\text{H}_2\text{O})_{10}^{3+}$ from $6+3 \text{La}(\text{H}_2\text{O})_9^{3+}$ in the course of a concerted water exchange.

It appears that a simple potential form describes correctly the $\text{La}^{3+}\text{-OH}_2$ interaction: the Buck-6 potential only composed of a repulsion and a dispersion term. This simplicity will facilitate, in the future, extrapolation of parameters we have determined for the La-O interaction to the other Ln-O interactions (Ln = Ce - Lu), since the Ln^{3+} hydration properties in aqueous solution depends essentially on the Ln^{3+} ionic radius, and our Buck-6 potential indeed essentially reflects ionic radius.

The present study encourages us to proceed further with other lanthanide ions hydration studies and with La^{3+} solvation in aqueous solutions containing anions and other cations.

Acknowledgments

We are grateful to Dr. Marie-Pierre Gaigeot for helpful discussions and suggestions. She initiated the project that produced the computer program used in the present work.

* Electronic address: pierre.vitorge@cea.fr

- [†] Also at Laboratoire Analyse et Modélisation pour la Biologie et l'Environnement, CNRS UMR 8587, Université d'Evry Val d'Essonne, Boulevard F. Mitterrand, 91025 Evry Cedex, France.
- ¹ W. Meier, P. Bopp, M. M. Probst, E. Spohr, and J. L. Lin, *J. Phys. Chem.* **94**, 4672 (1990).
- ² S. Galera, J. M. Lluch, A. Oliva, J. Bertran, F. Foglia, L. Helm, and A. E. Merbach, *New J. Chem.* **17**, 773 (1993).
- ³ L. Helm, F. Foglia, T. Kowall, and A. E. Merbach, *J. Phys.: Condens. Matter* **6**, A132 (1994).
- ⁴ T. Kowall, F. Foglia, L. Helm, and A. E. Merbach, *J. Phys. Chem.* **99**, 13078 (1995).
- ⁵ T. Kowall, F. Foglia, L. Helm, and A. E. Merbach, *J. Am. Chem. Soc.* **117**, 3790 (1995).
- ⁶ S. Chaussement and A. Monteil, *J. Chem. Phys.* **105**, 6532 (1996).
- ⁷ T. Kowall, F. Foglia, L. Helm, and A. E. Merbach, *Chem. Eur. J.* **2**, 285 (1996).
- ⁸ F. M. Floris and A. Tani, *J. Chem. Phys.* **115**, 4750 (2001).
- ⁹ A. Chaumont and G. Wipff, *Inorg. Chem.* **43**, 5891 (2004).
- ¹⁰ C. Clavaguéra, R. Pollet, J. M. Soudan, V. Brenner, and J. P. Dognon, *J. Phys. Chem. B* **109**, 7614 (2005).
- ¹¹ S. R. Hughes, T.-N. Nguyen, J. A. Capobianco, and G. H. Peslherbe, *Int. J. Mass Spectrom.* **241**, 283 (2005).
- ¹² C. Clavaguera, F. Calvo, and J.-P. Dognon, *J. Chem. Phys.* **124**, 074505 (2006).
- ¹³ A. Ruas, P. Guilbaud, C. Den Auwer, C. Moulin, J.-P. Simonin, P. Turq, and P. Moisy, *J. Phys. Chem. A* **110**, 11770 (2006).
- ¹⁴ B. M. Rode and T. S. Hofer, *Pure & Appl. Chem.* **78**, 525 (2006).
- ¹⁵ T. Ikeda, M. Hirata, and T. Kimura, *J. Chem. Phys.* **122**, 244507 (2005).
- ¹⁶ H.-S. Kim, *Chem. Phys. Lett.* **330**, 570 (2000).
- ¹⁷ A.-L. Derepas, J.-M. Soudan, V. Brenner, and P. Millié, *J. Comput. Chem.* **23**, 1013 (2002).
- ¹⁸ M. Souaille, D. Borgis, and M.-P. Gaijeot, *MDVRY: Molecular Dynamics Program Developed at the University of Evry* (2006) (for more information please contact Marie-Pierre Gaijeot at gaijeot@ccr.jussieu.fr).
- ¹⁹ L. Helm and A. E. Merbach, *Coord. Chem. Rev* **187**, 151 (1999).
- ²⁰ J.-P. Blaudeau, S. A. Zygmunt, L. A. Curtiss, D. T. Reed, and B. E. Bursten, *Chem. Phys. Lett.* **310**, 347 (1999).
- ²¹ T. Yang, S. Tsushima, and A. Susuki, *J. Phys. Chem. A* **105**, 10439 (2001).
- ²² P. Allen, J. J. Bucher, D. K. Shuh, N. M. Edelstein, and I. Craig, *Inorg. Chem.* **39**, 595 (2000).

- ²³ P. Lindqvist-Reis, R. Klenze, G. Schubert, and T. Fanghänel, *J. Phys. Chem. B* **109**, 3077 (2005).
- ²⁴ P. Lindqvist-Reis, C. Walther, R. Klenze, A. Eichhofer, and T. Fanghanel, *J. Phys. Chem. B* **110**, 5279 (2006).
- ²⁵ P. Vitorge, V. Phrommavanh, B. Siboulet, D. You, T. Vercoüter, M. Descostes, C. J. Marsden, C. Beaucaire, and J.-P. Gaudet, *Comptes Rendus Chimie*, **in press** (2007).
- ²⁶ R. Silva, G. Bidoglio, M. Rand, P. Robouch, H. Wanner, and I. Puigdomenech, *Chemical Thermodynamics of Americium* (OECD NEA Data Bank, Issy-les-Moulineaux, FRANCE, 1995).
- ²⁷ P. Vitorge and H. Capdevila, *Radiochim. Acta* **91**, 623 (2003).
- ²⁸ P. Vitorge, *Chimie des actinides (Chemistry of actinides)*, vol. BN2 (Techniques de l'ingénieur, Paris, FRANCE, 1999).
- ²⁹ J. Näslund, P. Lindqvist-Reis, I. Persson, and M. Sandström, *Inorg. Chem.* **39**, 4006 (2000).
- ³⁰ S.-I. Ishiguro, Y. Umebayashi, K. Kato, R. Takahashib, and K. Ozutsumi, *J. Chem. Soc. Faraday Trans.* **94**, 3607 (1998).
- ³¹ J. A. Solera, J. Garcia, and M. G. Proietti, *Phys. Rev. B* **51**, 2678 (1995).
- ³² G. Johansson and H. Wakita, *Inorg. Chem.* **24**, 3047 (1985).
- ³³ A. Habenschuss and F. H. Spedding, *J. Chem. Phys.* **70**, 3758 (1979).
- ³⁴ L. S. Smith and D. L. Wertz, *J. Am. Chem. Soc.* **97**, 2365 (1975).
- ³⁵ L. Helm and A. E. Merbach, *Chem. Rev.* **105**, 1923 (2005).
- ³⁶ C. Cossy and A. E. Merbach, *Pure & Appl. Chem.* **60**, 1785 (1988).
- ³⁷ C. Cossy, L. Helm, and A. E. Merbach, *Inorg. Chem.* **27**, 1973 (1988).
- ³⁸ P. Caravan and A. E. Merbach, *Chem. Commun.* **22**, 2147 (1997).
- ³⁹ H. Ohtaki, *Monatshefte für Chemie / Chemical Monthly* **132**, 1237 (2001).
- ⁴⁰ L. Helm and A. E. Merbach, *J. Chem. Soc., Dalton Trans.* pp. 633–641 (2002).
- ⁴¹ C. Cossy, L. Helm, and A. E. Merbach, *Inorg. Chim. Acta* **139**, 147 (1987).
- ⁴² C. Cossy, L. Helm, and A. E. Merbach, *Inorg. Chem.* **28**, 2699 (1989).
- ⁴³ D. P. Fay, D. Litchinsky, and N. Purdie, *J. Phys. Chem.* **73**, 544 (1969).
- ⁴⁴ R. V. Southwood-Jones, W. L. Earl, K. E. Newman, and A. E. Merbach, *J. Chem. Phys.* **73**, 5909 (1980).
- ⁴⁵ B. T. Thole, *Chem. Phys.* **59**, 341 (1981).
- ⁴⁶ P. van Duijnen and M. Swart, *J. Phys. Chem. A* **102**, 2399 (1998).

- ⁴⁷ *Handbook of Chemistry and Physics* (CRC Editor, 1996).
- ⁴⁸ R. Car and M. Parrinello, *Phys. Rev. Lett.* **55**, 2471 (1985).
- ⁴⁹ M. Sprik, *J. Phys. Chem.* **95**, 2283 (1991).
- ⁵⁰ J. E. Lennard-Jones, *Proc. Roy. Soc. A* **106**, 463 (1924).
- ⁵¹ W. L. Jorgensen, J. Chandrasekhar, J. D. Madura, R. W. Impey, and M. L. Klein, *J. Chem. Phys.* **79**, 926 (1983).
- ⁵² J. Caldwell, L. X. Dang, and P. A. Kollman, *J. Am. Chem. Soc.* **112**, 9144 (1990).
- ⁵³ J. W. Caldwell and P. A. Kollman, *J. Phys. Chem.* **99**, 6208 (1995).
- ⁵⁴ R. Armunanto, C. F. Schwenk, A. H. B. Setiaji, and B. M. Rode, *Chem. Phys.* **295**, 63 (2003).
- ⁵⁵ R. A. Buckingham, *Proc. Roy. Soc.* **168 A**, 264 (1938).
- ⁵⁶ F. G. Fumi and M. P. Tosi, *J. Phys. Chem. Solids* **25**, 31 (1964).
- ⁵⁷ M. P. Tosi and F. G. Fumi, *J. Phys. Chem. Solids* **25**, 45 (1964).
- ⁵⁸ A. I. Kitaygorodsky, *Tetrahedron* **14**, 230 (1961).
- ⁵⁹ A.-L. Derepas, Ph.D. thesis, Université Paris XI, FRANCE (2001).
- ⁶⁰ M. Frisch, G. Trucks, H. Schlegel, G. Scuseria, M. Robb, J. Cheeseman, V. Zakrzewski, J. Jr., R. Stratmann, J. Burant, et al., *Gaussian 98, Revision A.9* (1998), Gaussian, Inc., Pittsburgh PA.
- ⁶¹ P. J. Hay and W. R. Wadt, *J. Chem. Phys.* **82**, 270 (1985).
- ⁶² W. R. Wadt and P. J. Hay, *J. Chem. Phys.* **82**, 284 (1985).
- ⁶³ P. J. Hay and W. R. Wadt, *J. Chem. Phys.* **82**, 299 (1985).
- ⁶⁴ P. C. Hariharan and J. A. Pople, *Theoret. Chim. Acta* **28**, 213 (1973).
- ⁶⁵ U. Essmann, L. Perera, M. L. Berkowitz, T. Darden, H. Lee, and L. G. Pedersen, *J. Chem. Phys.* **103**, 8577 (1995).
- ⁶⁶ G. Hummer, L. Pratt, and A. Garcia, *J. Phys. Chem.* **100**, 1206 (1996).
- ⁶⁷ S. Bogusz, T. E. C. III, and B. R. Brooks, *J. Chem. Phys.* **108**, 7070 (1998).
- ⁶⁸ D. Frenkel and B. Smit, *Understanding Molecular Simulation* (Academic Press, New York, 1996).
- ⁶⁹ T. Matthey, *Plain Ewald and PME* (2005).
- ⁷⁰ M. Duvail, R. Spezia, T. Cartailleur, and P. Vitorge, *Chem. Phys. Lett.* **submitted** (2007).
- ⁷¹ R. W. Impey, P. A. Madden, and I. R. McDonald, *J. Phys. Chem.* **87**, 5071 (1983).
- ⁷² T. S. Hofer, H. T. Tran, C. F. Schwenk, and B. M. Rode, *J. Comput. Chem.* **25**, 211 (2004).

- ⁷³ A. Amadei, M. Aschi, R. Spezia, and A. Di Nola, *J. Mol. Liq.* **101**, 181 (2002).
- ⁷⁴ G. Chillemi, P. D'Angelo, N. Pavel, N. Sanna, and V. Barone, *J. Am. Chem. Soc.* **124**, 1968 (2002).
- ⁷⁵ A. K. Soper, *Chem. Phys.* **258**, 121 (2000).
- ⁷⁶ R. D. Shannon, *Acta Cryst. A* **32**, 751 (1976).
- ⁷⁷ M. Duvail, P. Vitorge, R. Spezia, and T. Cartailleur, **in preparation** (2007).
- ⁷⁸ S. Chaussement, A. Monteil, M. Ferrari, and L. D. Longo, *Phil. Mag. B* **77**, 681 (1998).
- ⁷⁹ H. Ohtaki and T. Radnai, *Chem. Rev.* **93**, 1157 (1993).
- ⁸⁰ G. Laurenczy and A. E. Merbach, *Helv. Chim. Acta* **71**, 1971 (1988).

TABLE I: Parameters used for the CLMD simulations. Energies are in $\text{kJ}\cdot\text{mol}^{-1}$, distances in \AA and atomic polarizabilities in \AA^3 .

ion/water	IP	ε_{O-O}	σ_{O-O}	A_{ij}	B_{ij}	$C_{6,ij}$	$C_{8,ij}$	$C_{10,ij}$	q_i	α
La^{3+}	Exp			$5.111 \times 10^{+5}$	3.50				+3.000	1.41
La^{3+}	Exp _{up}			$5.805 \times 10^{+5}$	3.86				+3.000	1.41
La^{3+}	Buck-6			$1.004 \times 10^{+6}$	3.48	$3.766 \times 10^{+4}$			+3.000	1.41
La^{3+}	Buck-6 _{up}			$1.046 \times 10^{+6}$	3.50	$3.975 \times 10^{+4}$			+3.000	1.41
La^{3+}	TF			$-6.576 \times 10^{+3}$	1.27	$-9.206 \times 10^{+4}$	$1.234 \times 10^{+5}$	$-1.745 \times 10^{+4}$	+3.000	1.41
La^{3+}	TF _{up}			$6.474 \times 10^{+5}$	3.06	$1.322 \times 10^{+5}$	$-2.821 \times 10^{+5}$	$2.210 \times 10^{+5}$	+3.000	1.41
La^{3+}	Kit			$2.309 \times 10^{+6}$	4.119	$3.843 \times 10^{+3}$	$9.205 \times 10^{+3}$	$2.976 \times 10^{+4}$	+3.000	1.41
O_w	TIP3P/P	0.510	3.165						-0.658	0.85
O_w	TIP3P	0.649	3.165						-0.834	0.85
O_w	Kit			$8.576 \times 10^{+5}$	3.984	$9.821 \times 10^{+2}$	$2.515 \times 10^{+3}$	$8.690 \times 10^{+3}$	-0.834	0.85
H_w	TIP3P/P								+0.329	0.41
H_w	TIP3P								+0.417	0.41

TABLE II: Hydration properties of La^{3+} in aqueous solution at room temperature.^a First ($r_{\text{La-O}}^{(1)}$) and second ($r_{\text{La-O}}^{(2)}$) maximum peak of La-O RDFs (in Å).^b Coordination number of the first ($\text{CN}^{(1)}$) and the second ($\text{CN}^{(2)}$) hydration shell.^c MRT of water molecule in the first ($\text{MRT}^{(1)}$) and the second ($\text{MRT}^{(2)}$) hydration shell (in ps).^d Present study with the TIP3P/P (polarizable) water model.^e Present study with the TIP3P (unpolarizable) water model.^f QM/MM MD.¹⁴^g MD on the $\text{La}(\text{H}_2\text{O})_{60}^{3+}$ cluster.¹⁰^h CPMD on LaCl_3 in aqueous solution.¹⁵ⁱ EXAFS (L_{II} - L_{III} edge) - 0.25 mol·L⁻¹ Cl⁻.²²^j EXAFS and LAXS (L_{II} edge) - 3.856 mol·L⁻¹ ClO₄⁻.²⁹^k EXAFS (L_{III} edge) - 0.8094 mol·L⁻¹ La(ClO₄)₃.³⁰^l EXAFS (L_{III} edge) - 0.05 to 0.20 mol·L⁻¹ LaCl₃.³¹^m XRD - 9.16 mol·L⁻¹ ClO₄⁻.³²ⁿ XRD - 3.808 mol·kg⁻¹ LaCl₃.³³^p XRD - 1.54 to 2.67 mol·kg⁻¹ LaCl₃.³⁴¹ Mean value of two different distances corresponding to a CN of 9 = 6+3.

	$r_{\text{La-O}}^{(1)a}$	$\text{CN}^{(1)b}$	$\text{MRT}^{(1)c}$	$r_{\text{La-O}}^{(2)a}$	$\text{CN}^{(2)b}$	$\text{MRT}^{(2)c}$
Exp ^d	2.59	8.77	201	4.85	22.4	8.7
Buck-6 ^d	2.52(2.50/2.58) ¹	9.02	1082	4.65	18.8	7.6
TF ^d	2.65	10.2	176	4.75	24.1	7.4
Kit ^d	2.55	8.76	207	4.83	21.4	5.7
Kit-TIP3P/P ^d	2.56	8.92	401	4.78	19.6	7.2
Exp _{up} ^e	2.46	9.02	610	4.60	18.1	7.5
Buck-6 _{up} ^e	2.56	10.0	910	4.70	20.4	7.1
TF _{up} ^e	2.62	12.0	998	4.75	26.3	7.9
QM/MM MD ^f	-	9-10	>250	-	18-28	8.4
MD ^g	2.56	8.90	980	4.68	15.9	-
CPMD ^h	2.52	8.5	-	-	-	-
EXAFS ⁱ	2.54	9.20	-	-	-	-
EXAFS ^j	2.56(2.515/2.64) ¹	9(6+3)	-	4.63	18	-
EXAFS ^k	2.545	9	-	-	-	-
EXAFS ^l	2.56	12	-	-	-	-
XRD ^m	2.57	8	-	4.7	13	-
XRD ⁿ	2.58	9.13	-	5	-	-
XRD ^p	2.48	8	-	4.7	-	-

Figure Captions

Figure1: Geometry of the $\text{La}-(\text{OH}_2)_8^{3+}$ complex in the square antiprism (D_{4d}) geometry used to parametrize the interaction potentials from *ab initio* calculations.

Figure2: La-O radial distribution functions (left panels) and coordination numbers (right panels) obtained for the different interaction potentials: (a) Exp, (b) Buck-6, (c) TF, (d) Kit and (e) Kit-TIP3P/P potentials.

Figure3: O-O radial distribution functions obtained for $\text{La}(\text{H}_2\text{O})_{216}^{3+}$ MD simulations with the Kit-TIP3P/P (solid line) and the the Kit (dash line) potentials.

Figure4: Some snapshots of reduced hydrated La^{3+} ion clusters extracted from MD simulations done in bulk water: a-b) $\text{La}(\text{H}_2\text{O})_9^{3+}$, c) $\text{La}(\text{H}_2\text{O})_{14}^{3+}$ and d) $\text{La}(\text{H}_2\text{O})_{24}^{3+}$.

Figure5: *Ab initio* (MP2) versus polarizable Buck-6 model total internal energies for various $\text{La}(\text{H}_2\text{O})_n^{3+}$ clusters (n=1-24).

Figure6: Top: Radial distribution functions of La-O (solid line), La-H (dash line) and CN (dash-dot line).

Bottom: Angular distribution function of O-La-O in the first hydration shell compared to ADF of the D_{3h} TTP geometry.

Figure7: La-O distance of selected water molecules as a function of the simulation time showing a synchronous water exchange between the *green* and the *pink* water molecules. a) Before the water exchange, the *green* and the two *gray* water molecules are in the medium triangle. b) During the water exchange, the *green* and the *pink* water molecules are at the same distance of La^{3+} . c) After the water exchange, the two *gray* water molecules are now included in the prism, and the *pink* water molecule is in the medium triangle (For clarity, two orientation views are shown).

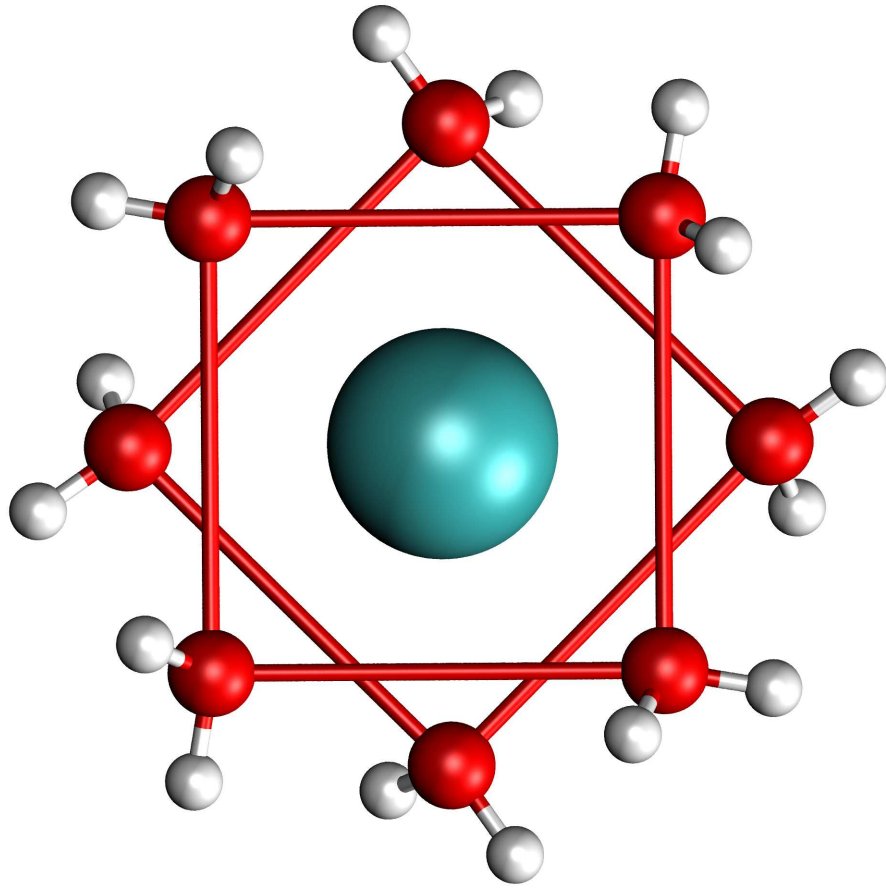


FIG. 1:

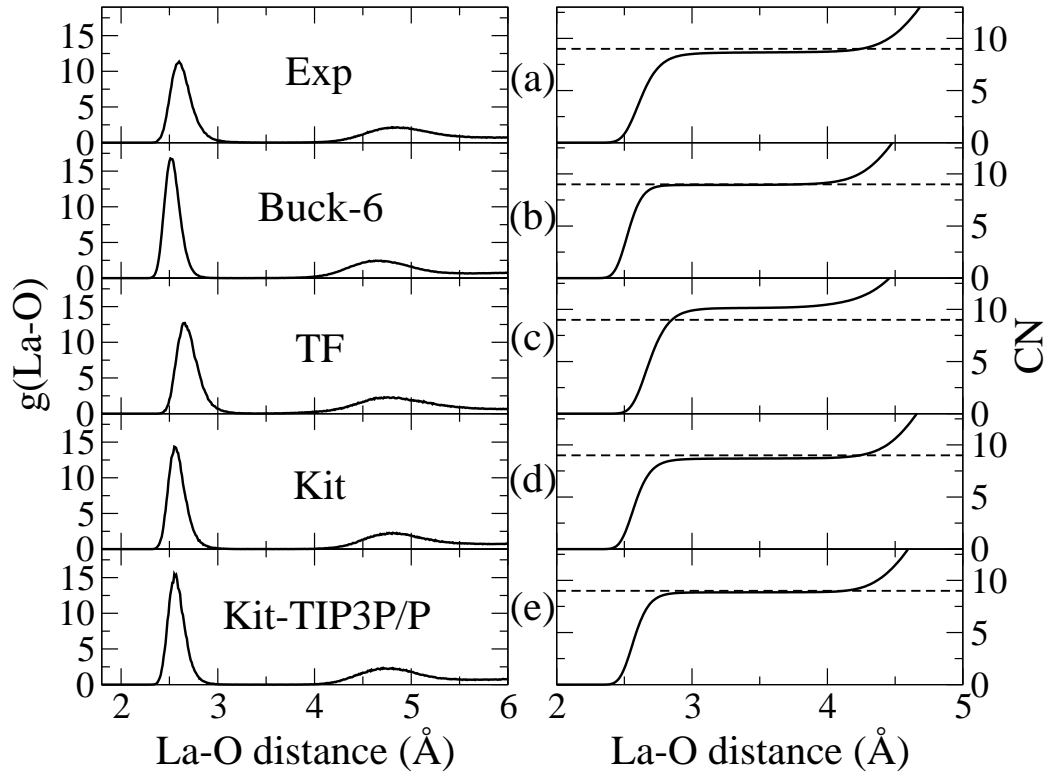


FIG. 2:

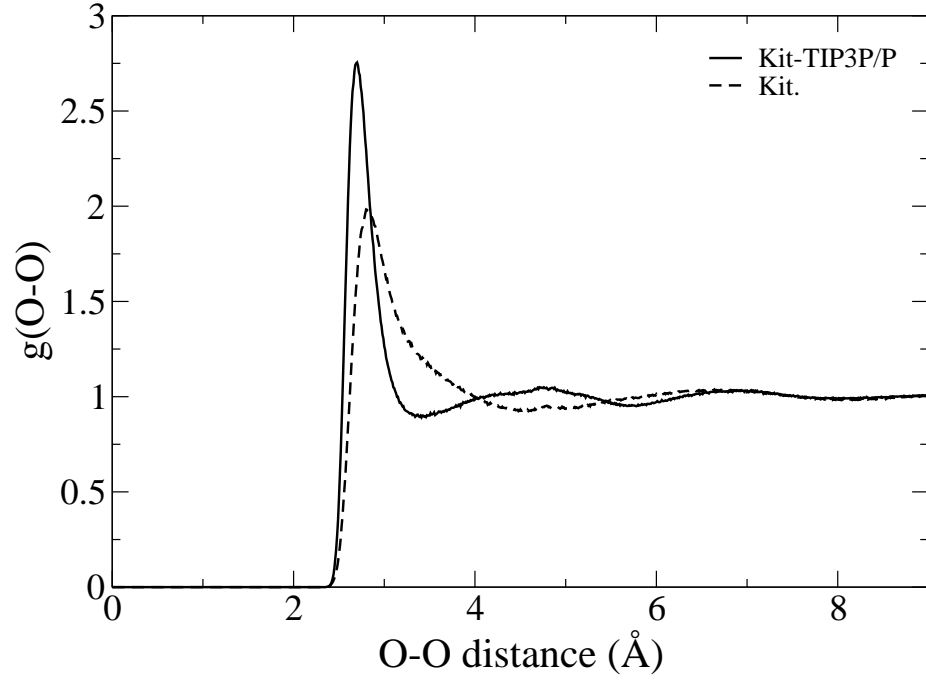


FIG. 3:

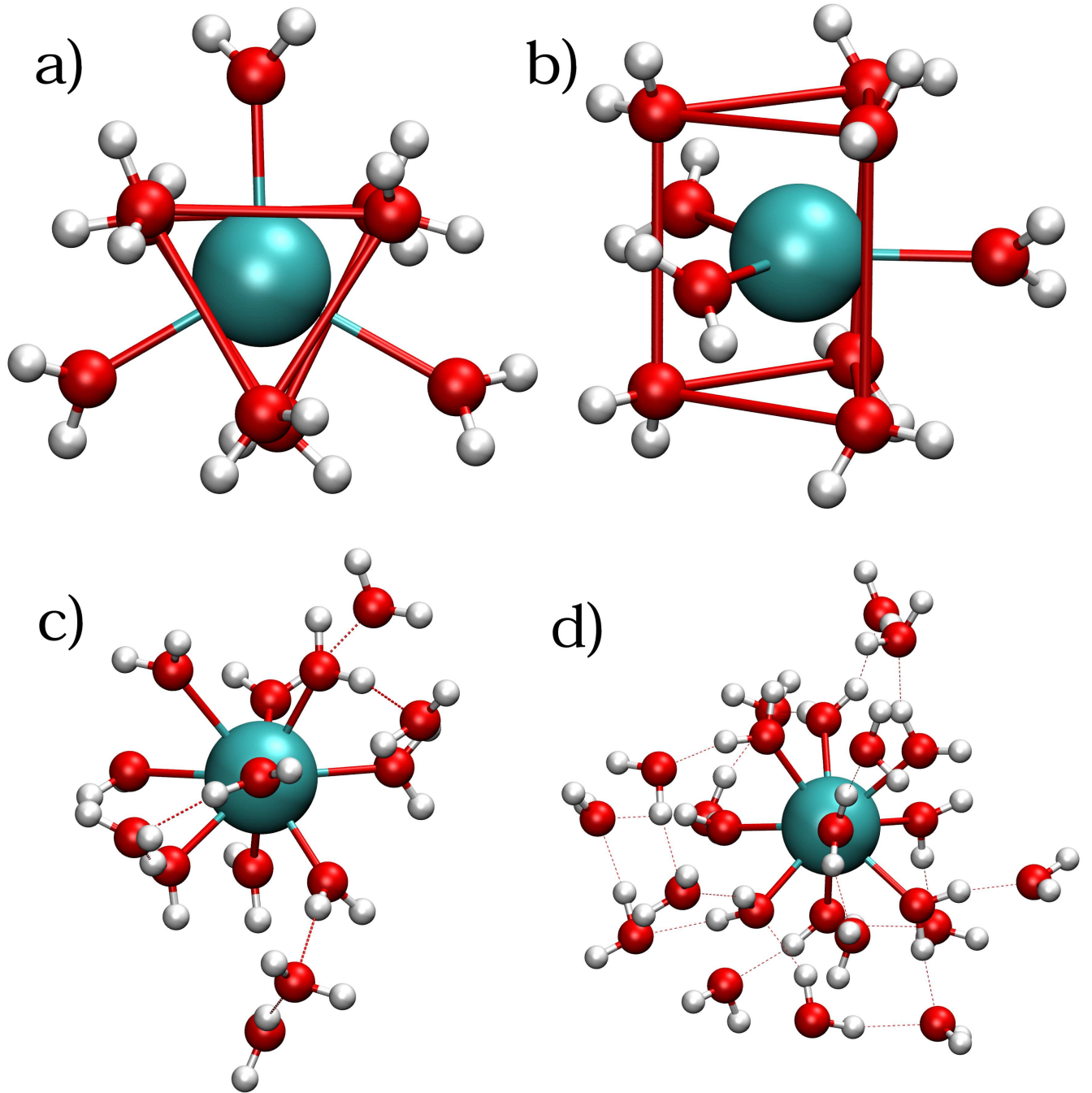


FIG. 4:

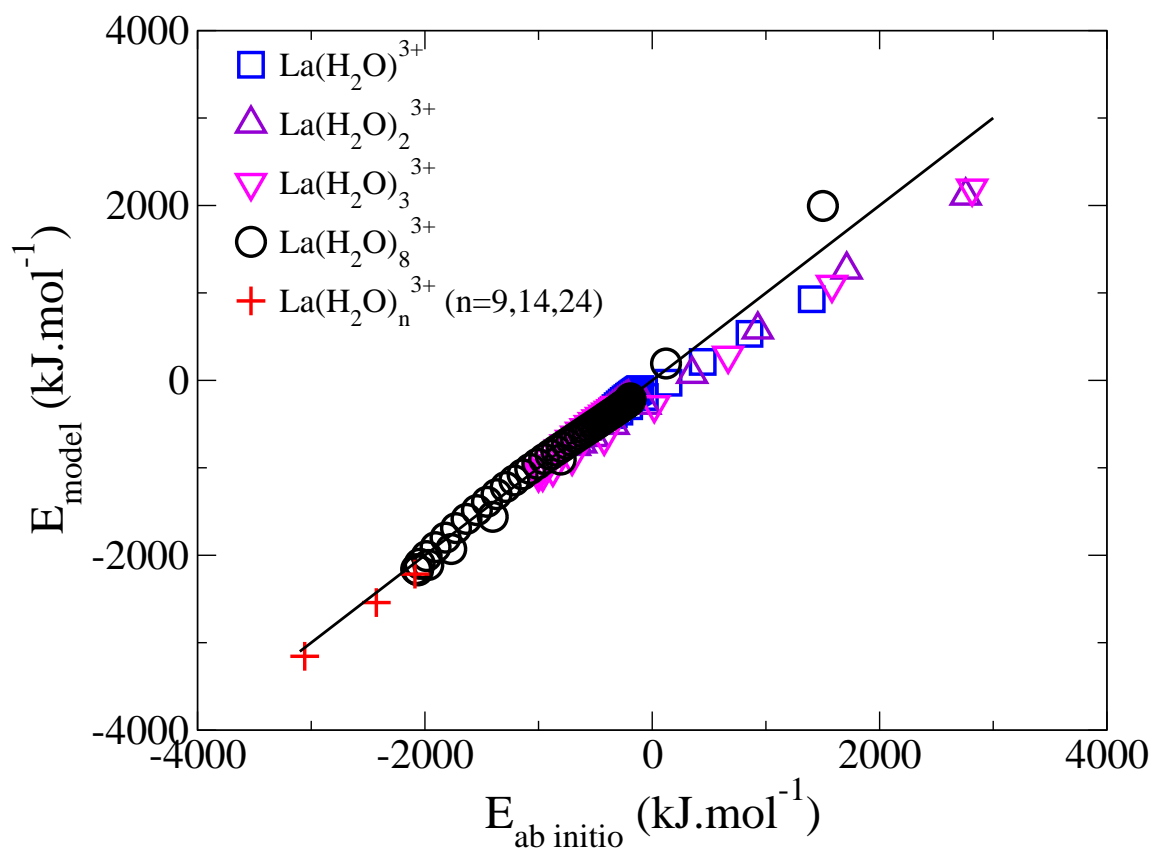


FIG. 5:

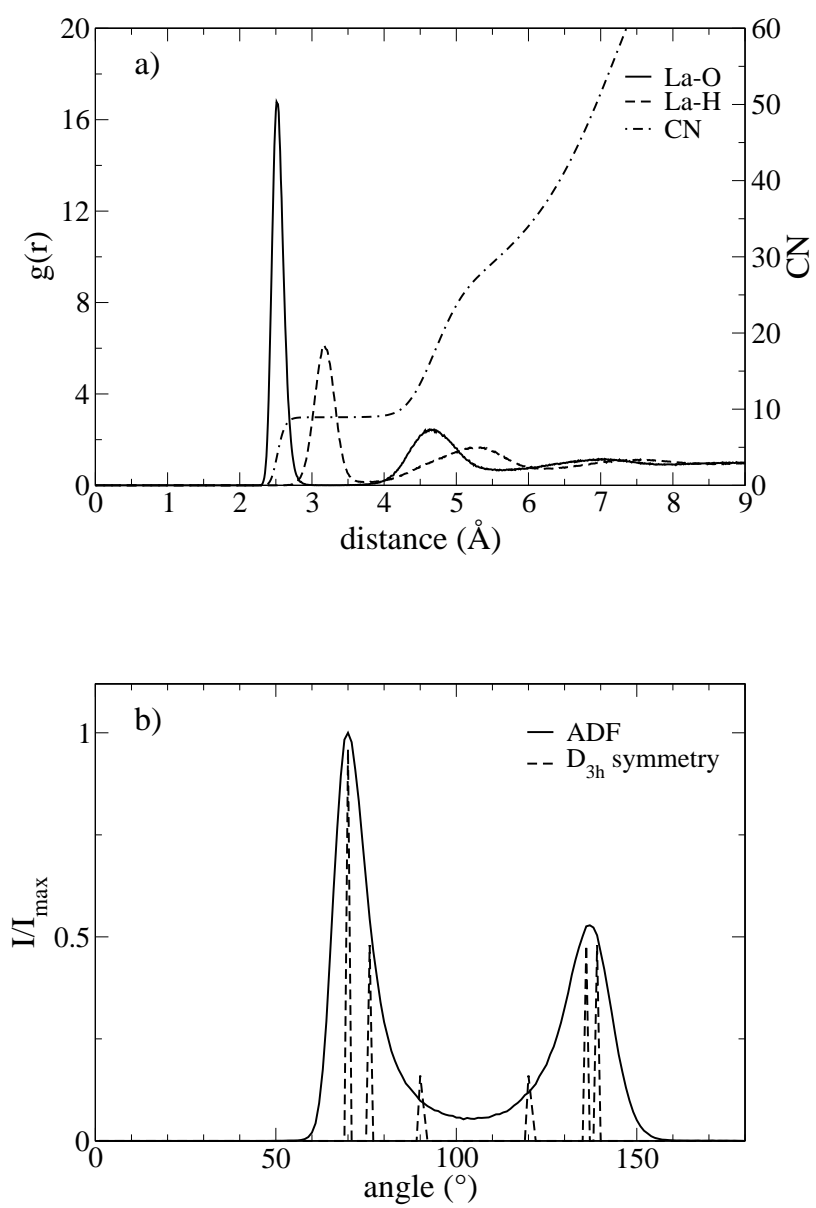


FIG. 6:

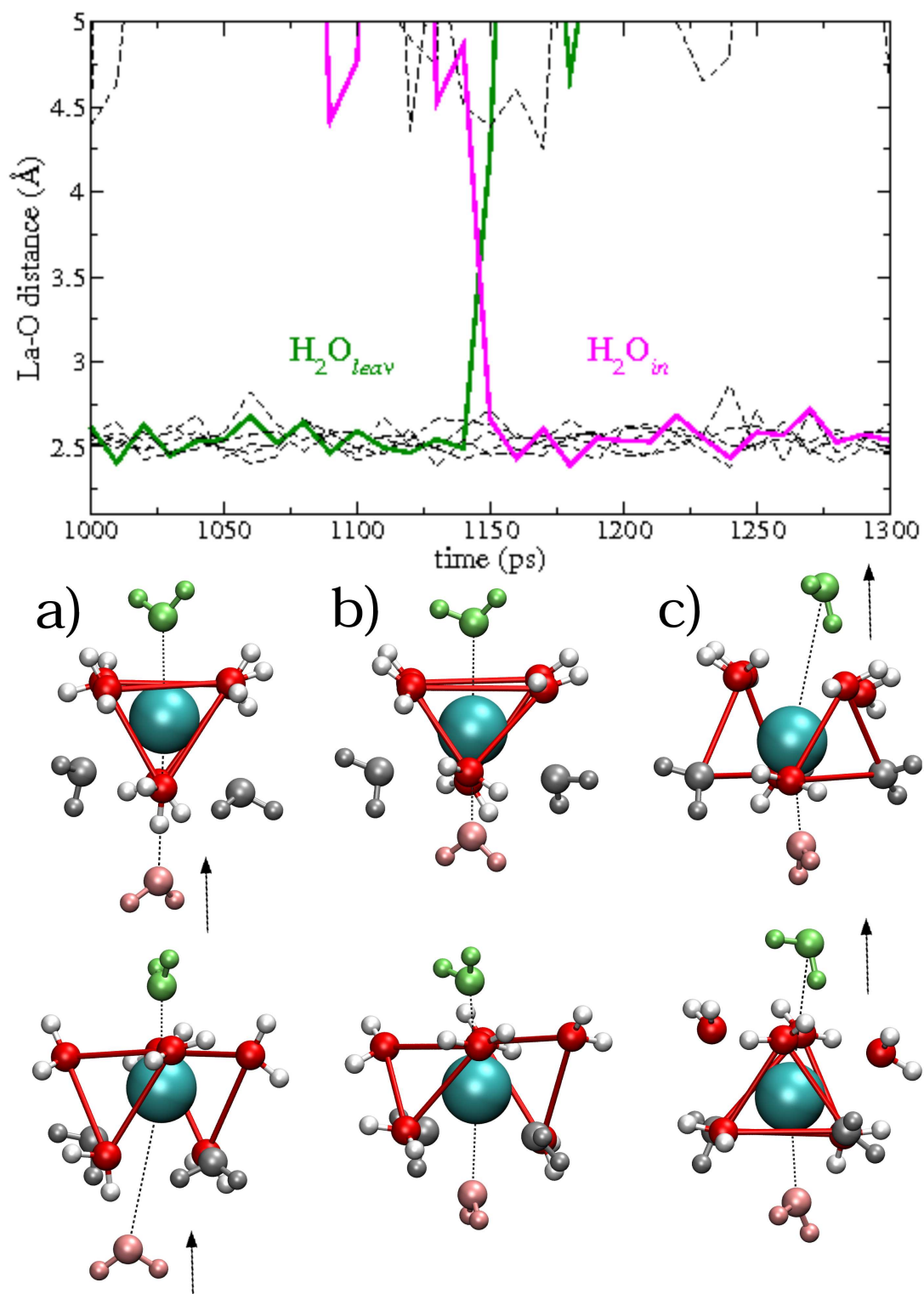


FIG. 7: